Nucleic Acids Research, 1996, Vol. 24, No. 8 **1443–1452**

Genomic position effects lead to an inefficient reorganization of nucleosomes in the 5′-regulatory region of the chicken lysozyme locus in transgenic mice

Matthias C. Huber, Gudrun Krüger and Constanze Bonifer*

Institut für Biologie III der Universität Freiburg, Schänzlestrasse 1, D-79104 Freiburg, Germany

Received January 18, 1996; Revised and Accepted March 1, 1996

ABSTRACT

The chicken lysozyme locus is gradually activated during macrophage development exhibiting a specific chromatin structure with each differentiation state. Its small size and the extensive characterization of its *cis*-regulatory elements allows us to study even subtle changes in chromatin structure of the entire gene locus during transcriptional activation. Tissue-specific and position independent expression of the lysozyme locus in transgenic mice requires the cooperation of all *cis*-regulatory elements. In order to elucidate further the molecular basis of locus activation, we have determined nucleosome positions within the complete 5′-regulatory region of the chicken lysozyme locus in chicken myeloid cell lines and transgenic mice. Each *cis*-regulatory element develops its unique nucleosomal structure and each one remodels chromatin differently. The nucleosomal organization of the endogenous gene in chicken cell lines and the transgene in the mouse turned out to be identical, enabling us to study the influence of *cis*-regulatory deletions on the development of an active chromatin structure in transgenic mice. Transgenes with a deletion of an important *cis*-regulatory element show an impediment in nucleosome reorganization as compared with the complete lysozyme locus. We demonstrate that multi-copy transgene-clusters in position dependently expressing mouse lines exhibit a heterogeneous chromatin organization.

INTRODUCTION

The organization of eukaryotic genes into nucleosomal arrays is not always random, but guided by proteins binding to specific DNA sequences and by the DNA sequence itself (1,2). It is assumed that nucleosomes contribute to the efficiency of transcription by generating a chromatin structure designed to interact with sequence-specific DNA-binding proteins in a highly specific fashion. It could be shown that the mutation of histone N-termini obstructs both the induction and repression of specific genes (3–5). Specifically positioned (phased) nucleosomes influence the accessibility of transcription factors to their recognition sequences (6–11). Consequently, chromatin structure has to be altered in order to allow binding and functional assembly of transcription factor complexes on enhancers and promoters. At the yeast PHO5 promoter induction of the gene is accompanied by a rearrangement of a nucleosome specifically positioned over a transcription factor binding site (6). A classic example is the MMTV promoter, where a nucleosome is phased at binding sites for the glucocorticoid receptor and the transcription factors NFI and OTF (8,10). However, here it could be shown that after binding of the transcription factors *in vivo* the nucleosome remains bound to DNA (12,13). Transcription factors seem to be bound on the nucleosomal surface, an arrangement which might be necessary for their precise spacial alignment (12,14). A similar arrangement was suggested for the active albumin enhancer (15).

Reorganization of chromatin structure upon transcriptional activation of gene loci is observed along an extended chromatin domain (16,17). Using the chicken lysozyme gene as a model, we demonstrated that a structurally defined chromatin domain also constitutes the regulatory unit of transcription. High level, tissue-specific and position independent expression of the lysozyme gene in transgenic mice requires the presence of the full set of *cis*-regulatory elements. Position independence of expression is lost whenever one essential *cis*-regulatory region is deleted (18,19), indicating a necessity for cooperation of all *cis*-regulatory elements. The activity of the various *cis*-regulatory elements on the lysozyme locus is indicated by the presence of DNase I hypersensitive sites (DHSs) in chromatin (20–22). We could show that position independently expressed transgenes form DHSs at the same position as in chicken macrophages. In contrast, in position dependently expressed transgenes with a low expression level per gene copy the formation of DHSs is suppressed (23). This indicates that at a chromosomal position unfavorable for gene expression the reorganization of chromatin normally leading to locus activation is disturbed. All mouse lines carry multiple transgene copies. For each mouse line the expression level in each cell as measured by RNA *in situ* hybridization is the same, raising the possibility that the reduced efficiency of DNase I hypersensitive site formation is the result of a variable ability of single loci within a multi-copy transgene cluster to form DHSs (23). In the experiments described here we addressed this question by analyzing the chromatin of

* To whom correspondence should be addressed

lysozyme transgenes expressed in a position dependent fashion by micrococcus nuclease (MNase) digestion. MNase preferentially cleaves in nucleosome linker regions (24), thus enabling the mapping of phased nucleosomes. We expected nucleosomes located around *cis*-regulatory elements to rearrange upon transcriptional activation. By comparing nucleosome phasing patterns between mouse lines we expected to get an unambiguous answer, because nucleosomes specifically phased on one DNA molecule occupy unambiguous positions.

The various *cis*-regulatory elements of the lysozyme locus and the *trans*-acting factors binding to these elements are well characterized. However, neither their nucleosomal organization nor the consequences of transcription factor interaction on nucleosome positioning has up to now been described. The elucidation of dynamic nucleosome rearrangements over an extended regulatory region provides the basis on which to study the molecular mechanism of the cooperative interaction of *cis*-regulatory elements. In addition, those studies were necessary in order to be able to correctly interpret chromatin structure studies in transgenic mice carrying deletion constructs. Therefore, we examined the nucleosomal organization of the entire 5′-regulatory region of the lysozyme locus in retrovirally transformed myeloid cell lines of the chicken representing various stages of macrophage development. We show that the 5′-regulatory region displays a highly ordered nucleosomal organization. We demonstrate that along with each macrophage differentiation step, nucleosomes at the various *cis*-regulatory elements are rearranged in an element-specific manner. The chromatin structure of lysozyme transgenes in mice carrying the complete set of *cis*-regulatory elements is undistinguishable from the endogenous gene in chickens. We were able, therefore, to study the effect of *cis*-regulatory deletions on the formation of active chromatin in transgenic mice. We demonstrate that multi-copy transgene clusters of deletion constructs exhibit a heterogeneous nucleosomal organization.

MATERIAL AND METHODS

Cell culture and transgenic mice

HD50 MEP cells (25) were grown in standard Eagle's MEM containing 8% fetal calf serum (FCS), 2% chicken serum (CS), 75 µg/ml conalbumin (Sigma), 0.03 i.U/ml insulin and 10^{-4} M β-mercaptoethanol. HD50 myl cells, HD37 cells (25) and HD11 cells (26) were grown in either Iscove's medium or DMEM containing 8% FCS and 2% CS. When indicated, the cells were stimulated with 5 µg/ml LPS (Sigma) for 24 h. Transgenic mice carrying chicken lysozyme domain constructs (19) were kept as homozygous lines in our own mouse colony. Primary macrophages were prepared from the peritoneal cavity of transgenic mice as described (18). For each assay, cells from 15–20 mice cultured in Iscove's medium supplemented with 10% FCS and 10% L-cell conditioned medium for 16 h (18). Macrophages were LPS stimulated as described above. Embryonic fibroblasts were prepared from day 12 mouse embryos by removing head and internal organs. The remaining tissue was digested with 0.25% collagenase (Sigma), 20% FCS in PBS for 1.5 h, single cells were cultured in standard Iscove's medium, 10% FCS and left in the incubator for 16 h.

Nuclei preparation

Nuclei were prepared by homogenizing cultured cells on ice with a Dounce homogenizer in buffer 1 (0.15 mM spermine, 0.5 mM spermidine, 15 mM Tris–HCl pH 7.5, 60 mM KCl, 15 mM NaCl, 2 mM EDTA, 0.5 mM EGTA and 500 mM sucrose, 1 mM PMSF) followed by centrifugation for 5 min at 1000 *g* at 4°C. Nuclei were washed once in buffer 2 (buffer 1 plus 0.5% Triton X-100), followed by a wash in buffer 3 (buffer 1 but with 350 mM sucrose instead of 500 mM). After this wash nuclei were centrifuged for 5 min at 600 *g* at 4°C.

DNase I and MNase digestion

Aliquots of 2×10^7 to 1×10^8 nuclei in ~100–200 µl buffer 3 nuclei were centrifuged for 5 min at 600 *g* at 4°C) and resuspended in buffer 4 (0.15 mM spermine, 0.5 mM spermidine, 15 mM Tris–HCl pH 7.5, 60 mM KCl, 15 mM NaCl, 0.2 mM EDTA, 0.2 mM EGTA). DNase I digestions were performed in 500 µl buffer 4. To 2×10^7 nuclei, 20 U (XS.0b) or 24 U (HD11) DNase I (Boehringer) were added. Digestion was started by adding 4 mM $MgCl_2$ and 2 mM $CaCl_2$. Incubations (15 min, 4°C) were stopped by adding 10 µl 0.5 M EDTA. MNase digestions were performed in 200 µl of buffer 4. For 2×10^7 nuclei, 0, 60, 200 U MNase (Pharmacia) were used. Digestion was started by adding 10 µl $CaCl_2$ (100 mM). Incubations (5 min, 25°C) were stopped by adding 10 µl 0.5 M EDTA. Digestions of genomic DNA with MNase were performed in 150 µl 10 mM Tris–HCl pH 7.5 with 0.14–27 U/ml. Incubations (15 min at 25°C) were started by adding 15 µl 10 mM $CaCl_2$ and stopped with 15 µl 50 mM EDTA. After DNase I or MNase digestion, nuclei were lysed in 500 µl 50 mM Tris–HCl pH 8.0, 2 mM EDTA, 0.2% SDS, 0.5 mg/ml Proteinase K and incubated overnight at 37°C. RNase (0.2 mg/ml) was added, after an incubation for 1 h at 37°C, the DNA was precipitated three times with ethanol. Digested DNA was restricted and at least 20–30 µg of fragmented DNA per slot were loaded on 10 mm thick vertical 1.5% agarose gels. The DNA was transferred to Biodyne B membranes and the filter was hybridized with an appropriate probe for indirect endlabelling. Probe 1 is a *Dra*I–*Bam*HI fragment (+255 to +600 bp), probe 2 is a *Sph*I–*Spe*I fragment (–3163 to –2906 bp), probe 3 is a *Pst*I–*Hin*dIII fragment (–1564 to –1429 bp), probe 4 is a *Dra*II–*Sph*I fragment (–3424 to –3163 bp), probe 5 is a *Hin*dIII–*Spe*I fragment (–2718 to –2906 bp), probe 6 is a *Sac*I–*Bam*HI fragment (–6492 to –6331 bp).

RESULTS

The chromatin structure of the chicken lysozyme gene is rearranged during macrophage differentiation

The chicken lysozyme locus is regulated by a set of well characterized *cis*-regulatory elements each responsible for a distinct subaspect of tissue specificity of expression (27–33). Using retrovirally transformed myeloid cell lines of the chicken representing various stages of macrophage differentiation (25,26,34) we previously determined the DHS pattern of the endogenous lysozyme gene (35). E26 transformed multipotent myeloid progenitor cells (MEPs) are transcriptionally inactive and exhibit the DHS pattern of the inactive gene locus as found in the erythroid cell line HD37 or primary cells which do not transcribe the gene (20). The only DHS formed in the region analyzed is located at the silencer element 2.4 kb upstream of the transcriptional start site. While this work was in progress, a new DHS at –3.9 kb was discovered (36). Preliminary experiments indicate that this region displays enhancer activity in myeloid cells (C. Bonifer, unpublished results). Along with the onset of transcription at the myeloblast stage represented by HD50 myl

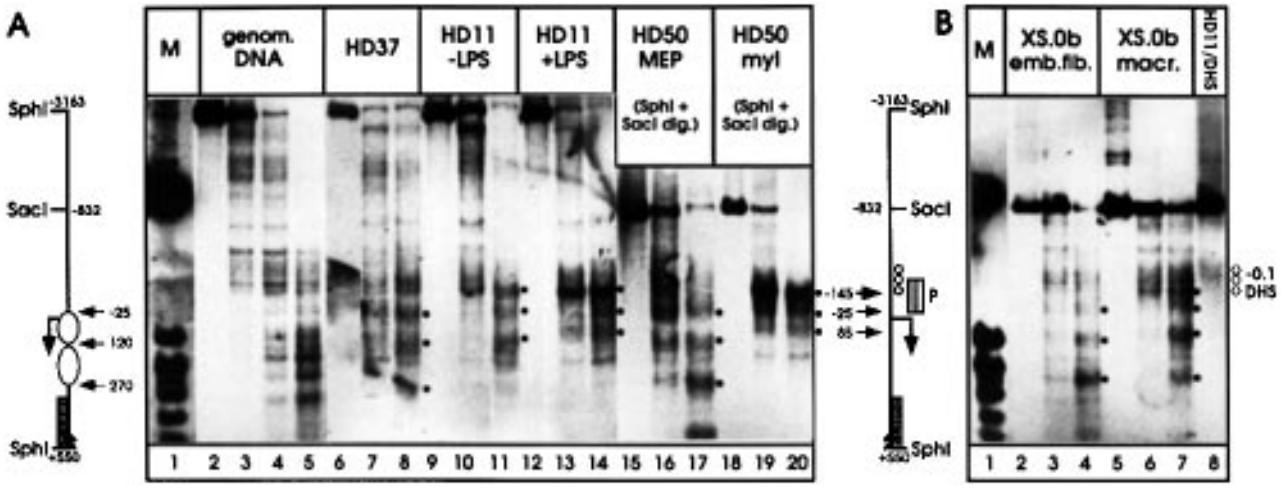

Figure 1. MNase analysis of the promoter region. (**A**) Lanes 2–5, MNase digestion pattern of naked genomic DNA; lanes 6–20, analysis of chicken cell lines. Genomic DNA isolated from MNase digested nuclei as well as control genomic DNA was analyzed after digestion with*Sph*I (lanes 6–13) or *Sph*I and *Sac*I (lanes 15–20). The deduced nucleosomal organization in transcriptionally inactive cells is indicated at the left, that of fully active cells at the right. (**B**) Lanes 2–7, MNase analysis of embryonic fibroblast (lanes 2–4) and macrophage nuclei (lanes 5–7) from transgenic mice XS.0b (Fig. 5); lane 8, the DHS (symbolized by small open circles) of HD11 nuclei in the analyzed region. Genomic DNA was restricted with *Sph*I and *Sac*I. Probe 1 was used for indirect endlabelling in (A) and (B); its position is indicated by a stippled box. The maps depicted in (A) are also applicable for (B). The immediate promoter region harboring the three transcriptional start sites and the enhancer is symbolized by a striped box. The positions of specific MNase cuts not present in genomic DNA (closed circles) are indicated on the map (black arrows). Large black arrows mark the positions of strong MNase cleavage sites in chromatin. Cleavage site positions indicated on the map are mean values of at least three experiments. Distances between MNase cleavage sites of 150–200 bp were taken as indication for phased nucleosomes (symbolized by open circles). M: Size marker.

cells, DHSs are formed at the promoter, at –3.9 kb (35) and at the upstream enhancer located at –6.1 kb. The transcriptional level is increased in subsequent differentiation steps, represented by the promacrophage cell line HD11. Expression is highest in LPS stimulated HD11 cells, which represent activated macrophages. Simultaneously, the DHS at the –2.4 kb silencer disappears and a new DHS at the –2.7 kb enhancer appears. LPS stimulated HD11 cells display an additional DHS at the hormone responsive element (HRE) located at –1.9 kb.

The chromatin fine structure of the 5′ regulatory region of the chicken lysozyme locus is conserved between the endogenous gene in chicken cells and transgenic mice

One way to investigate the influence of chromatin structure on transcription factor binding and locus activation is to manipulate and to reintroduce the respective DNA-sequences as a transgene. However, this requires that the chromatin structure observed at the endogenous gene of the donor species reforms in the new host. To this end, we compared the pattern generated by micrococcal nuclease (MNase) digestion of chromatin of the 5′-regulatory region of a position independently expressed lysozyme transgene (XS.0b; Fig. 5) in non-expressing embryonic fibroblasts as well as in macrophages to the pattern observed in chicken cell lines (Figs 2B–5B). The comparison demonstrates that the chromatin structure in non-expressing and expressing cells is highly conserved between chicken and mouse. Only at the region around the –3.9 kb DHS differences in the MNase pattern are observed (Fig. 3A and B). A series of bands is observed, indicating a mixed pattern derived from differently organized loci within the multi-copy transgene cluster. The DHS is located at the same position in chicken cells and mouse macrophages, but appears to be weaker (Fig. 3B, lanes 7 and 8). At all other *cis*-regulatory elements the same chromatin structure observed with the endogenous gene of the chicken is formed in the mouse.

Nucleosomal structure of the lysozyme promoter

The lysozyme promoter drives transcription in oviduct and macrophages, thereby interacting with different *cis*-regulatory elements. Three different mRNA initiation sites at +1/–2, –24 and –58 bp are used with the same relative frequency in both lysozyme expressing tissues (32,37). A myelomonocytic-specific enhancer element is located between –66 and –208 bp (31). Macrophage-specific *in vivo* protein–DNA interactions have been mapped around –200 bp, whereas protein–DNA contacts shared by oviduct and macrophages are located between –60 and –120 bp, most likely due to binding of Sp1 (38). One functional binding site for CCAAT/enhancer binding protein (C/EBP) (39) has been located between –193 and –208 bp (40). We mapped the position of MNase cleavage sites in the chromatin of the promoter region in HD50-MEP-, HD37-, HD50 myl-, HD11-cells and LPS stimulated HD11-cells (Fig. 1A) as well as in cells derived from transgenic mice (Fig. 1B). Purified genomic DNA digested to the same extent served as control. In transcriptionally inactive cells, three chromatin-specific MNase cuts were found around the transcriptional start site (Fig. 1A, lanes 6–8 and 15–17; Fig. 1B, lanes 2–4) which are indicative for the presence of two specifically positioned nucleosomes in this region. Figure 1B, lane 8 shows a DNase I digest of HD11 chromatin in order to compare the positions of DHS and MNase cleavage sites. The DHS consists of three sub-bands between –145 and –300 bp (41). The MNase cleavage pattern is changed upon transcriptional activation of the gene in HD50 myl and HD11 cells (Fig. 1A, lanes 9–14 and 18–20; Fig. 1B, lanes 5–7). A MNase hypersensitive site develops downstream of the DHS at position –145 bp, simultaneously the bands at –25, +120

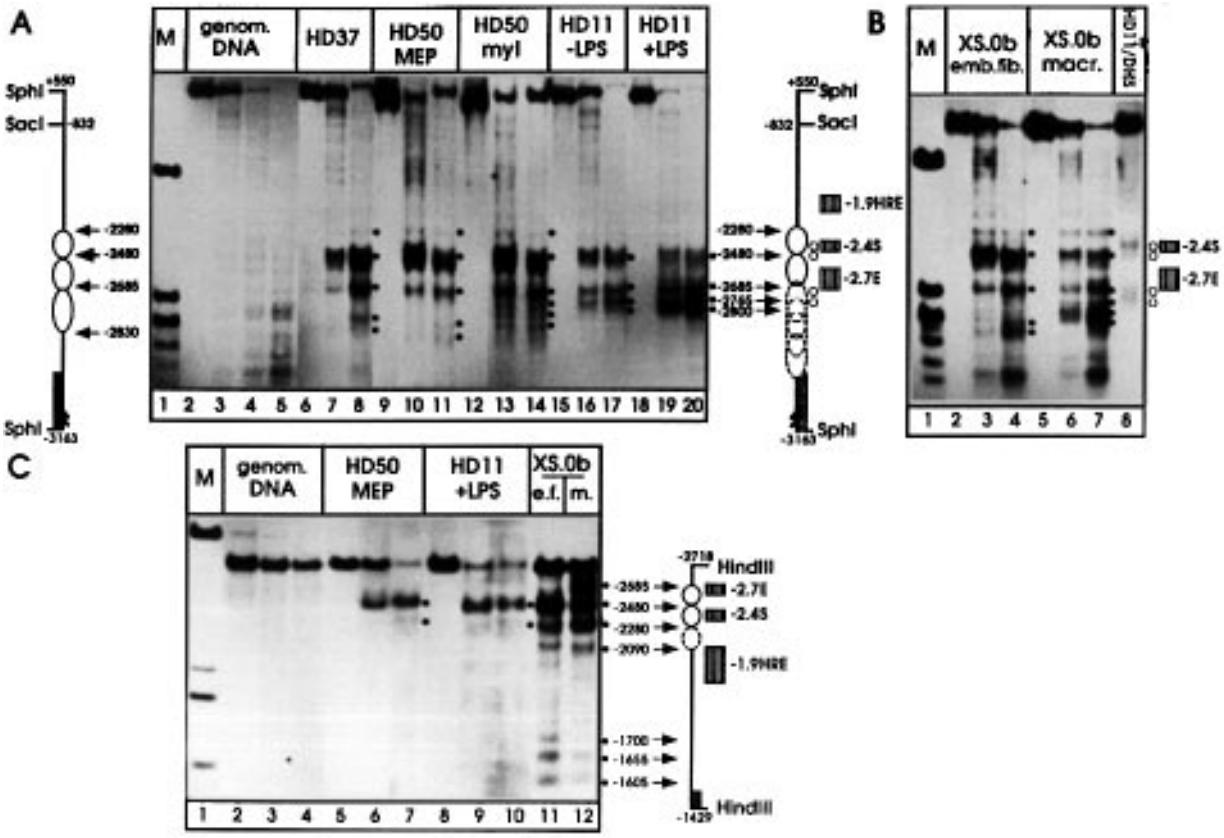

Figure 2. MNase analysis of the medial enhancer region. (**A**) Lanes 2–5, MNase digestion pattern of naked genomic DNA; lanes 6–20, analysis of chicken cell lines. DNA of MNase digested nuclei as well as genomic DNA was restricted with *Sph*I. The deduced nucleosomal organization of transcriptionally inactive cells is indicated at the left, that of fully active cells at the right. The positions of enhancer and silencer elements are indicated by striped boxes. (**B**) Lanes 2–7, MNase analysis of embryonic fibroblast (lanes 2–4) and macrophage nuclei (lanes 5–7) from transgenic mice XS.0b (Fig. 5); lane 8, a DHS analysis of HD11 nuclei of the same region. Isolated genomic DNA was restricted with *Sph*I and *Sac*I. Probe 2 was used for indirect endlabelling in (A) and (B); its position is indicated by a stippled box. The maps depicted in (A) are also applicable for (B). (**C**) MNase digestion analysis of chicken (lanes 5–10) and transgenic mouse cell chromatin (lanes 11 and 12) at lower resolution. Isolated genomic DNA was restricted with *Hin*dIII. Probe 3 was used for indirect endlabelling. The map on the right shows the deduced nucleosomal pattern of transcriptionally active cells. All other symbols: see legend of Figure 1.

and +270 bp disappear, indicating remodelling of nucleosomes at these positions.

The active –2.4 kb silencer and the active –2.7 kb enhancer are localized within an extended array of phased nucleosomes

The medial enhancer region consists of three major *cis*-regulatory elements, the HRE at –1.9 kb, the –2.4 kb silencer element and the –2.7 kb enhancer. The silencer element extends from –2410 to –2310 bp (28) and carries binding sites for two different proteins: the 5′-site is recognized by an abundant nuclear protein, NeP1; the 3′-site is a recognition sequence for thyroid hormone receptors (27,28,42). The –2.7 kb enhancer element extends from –2690 to –2540 bp (31,43) and carries an AP1 binding motif as well as binding sites for PU.1 (ets-family) (33,43) and C/EBP (44; Faust, N., Bonifer, C. and Sippel, A.E., submitted). *In vivo* footprinting experiments revealed only one DNA–protein contact at the PU.1 binding site at –2643 bp (33). The role of the –1.9 kb HRE in myeloid cells remains hereto unclear. No LPS responsive element has been identified at this position. LPS responsiveness of the chicken lysozyme gene rather seems to be mediated by C/EBP and NFκB binding sites located at the two enhancers and at the promoter (44,45). The MNase cleavage pattern at the medial enhancer region in chicken and mouse cells is depicted in Figure 2A, B and C. Indirect endlabelling with a probe hybridizing downstream of the HRE (Fig. 2C) revealed several chromatin specific MNase cuts indicative for the presence of phased nucleosomes. Three MNase generated bands at –2090, –2280 and –2480 bp respectively, are observed in all cells. No differences in MNase accessibility are observed around the HRE in LPS stimulated HD11 cells as compared with unstimulated cells. A structural difference between transcriptionally active and inactive cells, an additional band at –2685 bp, can be observed only in mouse macrophages, possibly due to a stronger hybridization signal as a consequence of high transgene copy number. However, a probe hybridizing at closer distance and thus examining this area at higher resolution revealed significant chromatin changes upon cellular differentiation also in chicken cells (Fig. 2A and B). MNase shows only a weak preference to certain sequence motifs in genomic DNA as compared with chromatin. In transcriptionally inactive cells the dominant MNase cleavage site seen at lower resolution (Fig. 2C) is composed of two closely spaced sites around –2480 bp. Two additional preferential cleavage sites are present at –2685 and –2830 bp. The

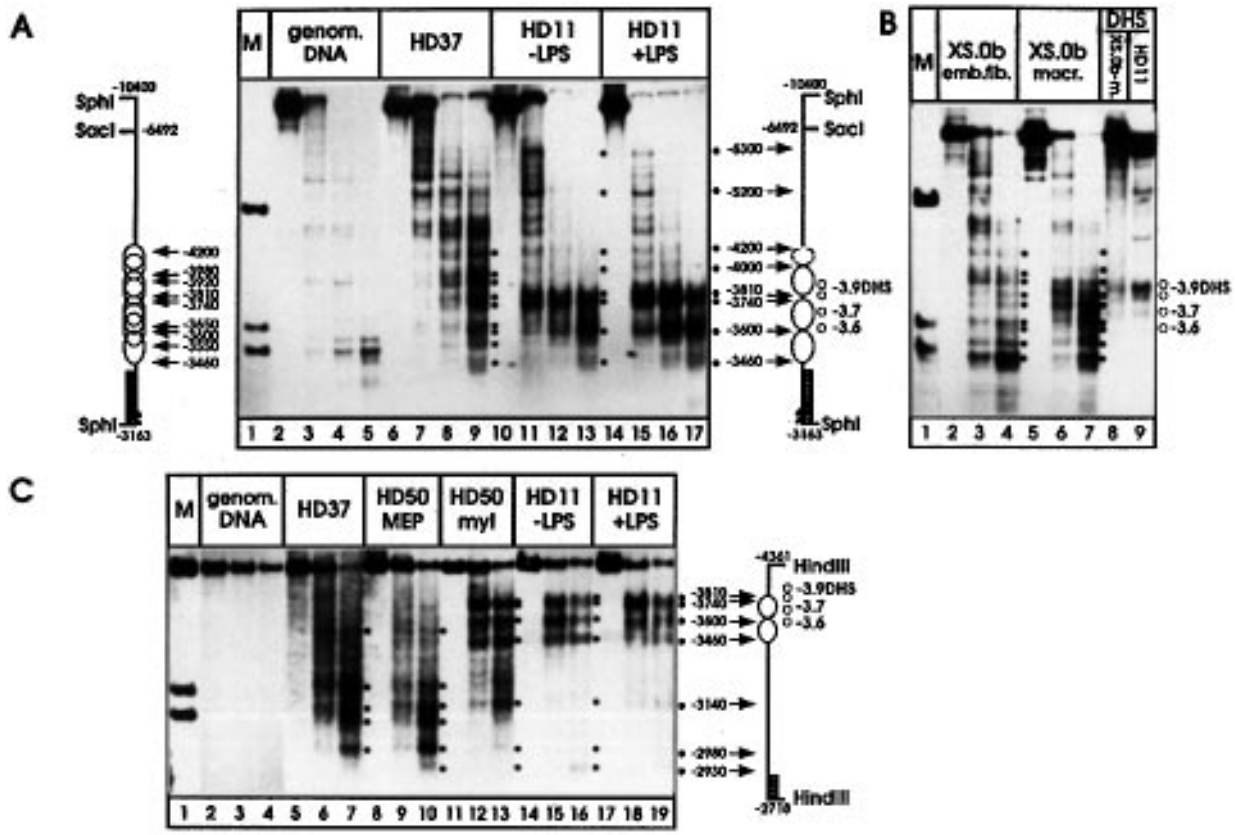

Figure 3. MNase analysis of the –3.9 kb enhancer. (**A**) Lanes 2–5, MNase digestion pattern of naked genomic DNA; lanes 6–17, analysis of chicken cell line chromatin. Isolated DNA was restricted with *Sph*I. The deduced nucleosomal organization of transcriptionally inactive cells is indicated at the left, that of fully active cells is indicated at the right. (**B**) Analysis of mouse embryonic fibroblasts (lanes 2–4) and macrophages (lanes 5–7) from mouse line XS.0b. Lanes 8 and 9 show a DHS analysis of HD11 and mouse macrophage nuclei. MNase and DNase I digested DNA was restricted with*Sph*I and *Sac*I and hybridized with Probe 4 [in (A) and (B)]. The maps depicted in (A) are also applicable for (B). (**C**) MNase digestion analysis of chicken cell line nuclei performed at lower resolution. DNA was isolated and restricted with *Hin*dIII and analyzed by indirect endlabelling with probe 5. The map on the right shows the deduced nucleosomal pattern of transcriptionally active cells. All other symbols: see legend of Figure 1.

distances between the cleavage sites indicate the presence of at least three phased nucleosomes (Fig. 2A). Upon cellular differentiation of MEPs into myeloblasts chromatin between –2685 and –2830 bp reorganizes at least in some cells, as indicated by the appearance of several new MNase generated cuts, suggesting a combination of the pattern found in transcriptionally active and inactive cells (Fig. 2A, lanes 12–14). The formation of a visible DHS in HD11 cells at –2.7 kb is accompanied by an increasing accessibility of these cleavage sites and a simultaneously decreasing accessibility of the cleavage sites at –2480 and –2830 bp (Fig. 2A, lanes 15–17). Upon LPS stimulation of HD11 cells, two strong MNase generated cuts appear upstream of the –2.7 kb enhancer at –2765 and –2800 bp (Fig. 2A, lanes 18–20). The same chromatin structure is found in transgenic mouse macrophages (Fig. 2B, lanes 5–7). For comparison, a DNase I digest of the chromatin of HD11 cells is shown (Fig. 2B, lane 8). Surprisingly, the DNase I cleavage sites at the –2.7 kb enhancer did not coincide with the *cis*-acting element mapped by transfection analysis. They overlap the position of the PU.1 binding site at –2643 bp and are mostly located upstream of the enhancer element. Our results indicate that in transcriptionally inactive cells the –2.4 kb silencer/–2.7 kb enhancer region is organized in a nucleosomal array of at least four phased nucleosomes (see also Fig. 2B and C), two of which are placed precisely over the *cis*-regulatory elements. In transcriptionally active cells the nucleosome located between –2685 and –2830 bp is destabilized. The nucleosomes covering the –2.4 kb silencer- and the –2.7 kb enhancer-elements are not relocated after onset of transcription, the dominant MNase cleavage sites at –2280, –2480 and –2685 bp still persist, even after LPS stimulation.

At the –3.9 kb enhancer, nucleosome phasing is induced upon transcriptional activation

The –3.9 kb region contains an enhancer element, however, its character and role in lysozyme gene regulation has not yet been clearly investigated. *In vitro*, binding of nuclear factor I (NFI) at –3880 bp has been demonstrated (46). The chromatin analysis of transcriptionally inactive cells at low resolution revealed no regularly spaced MNase pattern, however, nucleosomes are phased upon transcriptional activation of the lysozyme locus (Fig. 3C). Higher resolution analysis of transcriptionally inactive cells revealed a pattern of closely spaced MNase sites from –3460 to –4200 bp in HD37 cells (Fig. 3A, lanes 6–9; Fig. 3B, lanes 2–4). This pattern is radically changed in transcriptionally active cells (Fig. 3A, lanes 10–17; Fig. 3B, lanes 5–7). Strong regularly

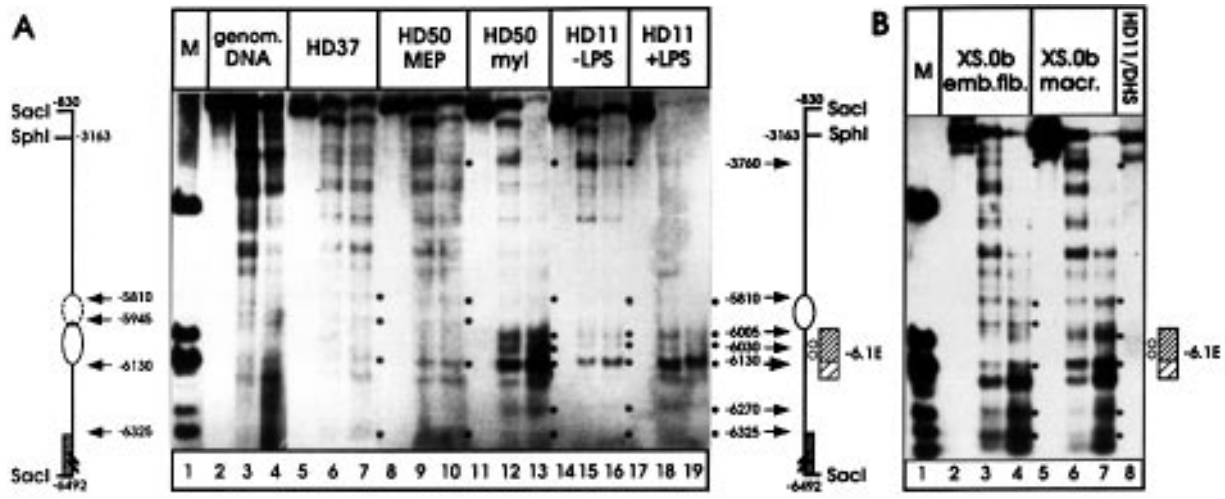

Figure 4. MNase analysis of the –6.1 kb enhancer region. (**A**) Lanes 2–4, MNase digestion pattern of naked genomic DNA; lanes 5–19, analysis of chicken cell line chromatin. The deduced nucleosomal organization of transcriptionally inactive cells is indicated at the left, that of fully active cells at the right. (**B**) Lanes 2–7, MNase analysis of embryonic fibroblast (lanes 2–4) and macrophage nuclei (lanes 5–7) from transgenic mice XS.0b. Lane 8 shows a DHS analysis of HD11 nuclei. Genomic DNA was digested with *Sac*I (A) or *Sac*I and *Sph*I (B) and analyzed by indirect endlabelling with probe 6. The maps depicted in (A) are also applicable for (B). The position of the –6.1 kb enhancer is indicated by the striped box, which is subdivided into the minimal enhancer (narrow stripes) and upstream regions carrying the second NFI binding site. All other symbols: see legend of Figure 1.

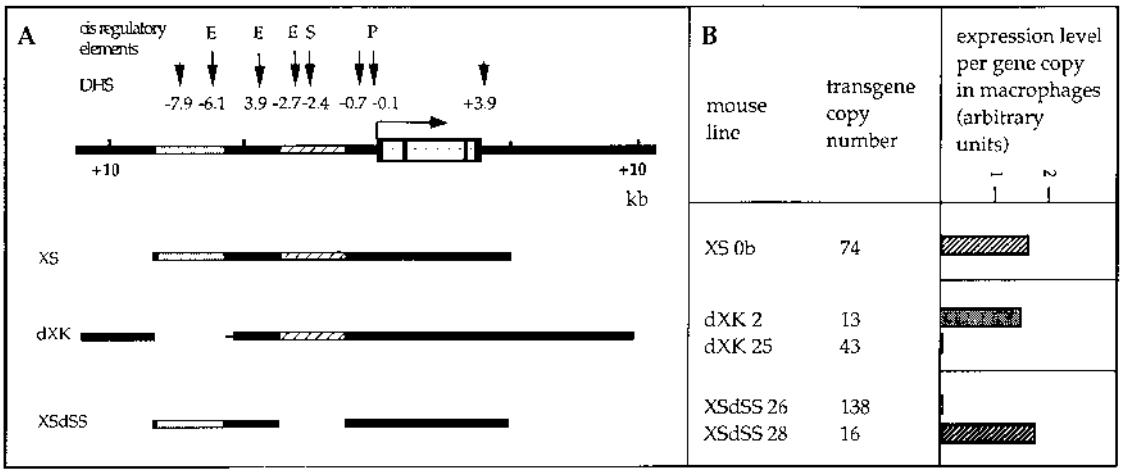

Figure 5. Mouse lines carrying deletion mutants of the chicken lysozyme gene domain used for chromatin analysis. (**A**) Map of the lysozyme locus showing the coding region indicated by the stippled box with the exon sequences drawn as black bars and the transcriptional start site as horizontal arrow. The positions of the DHSs mapped in macrophages are shown as vertical arrows, constitutive DHSs are indicated as smaller arrows. The position of the upstream and the medial enhancer region are indicated as striped boxes. The *cis*-regulatory elements and their position are shown in the uppermost panel. E: enhancer element; S: silencer element; P: promoter elements. Constructs used to generate transgenic mice are depicted below the genomic map. (**B**) Names of the five different mouse lines, their transgene copy number and expression levels per gene copy in macrophages. Construct XS is expressed in a position independent manner, all other constructs are expressed at variable levels.

spaced chromatin specific MNase cuts appear at –3810, –3740, –3600 and –3460 bp in chicken cells. The DHS analysis (Fig. 3B, lane 9) reveals several bands, the main cleavage site overlaps the NFI binding site. These results indicate the presence of an array of at least three phased nucleosomes forming between –4000 and –3460 bp, suggesting that a large DNA–protein complex blocks random nucleosome localization on this element.

The upstream enhancer reorganizes chromatin differently than the –2.7 kb enhancer upon activation

The –6.1 kb enhancer (32) is the best characterized regulatory element on the chicken lysozyme locus. Transfection analysis located enhancing activity on a minimal fragment (–6075 to –5918 bp) (29) comprised of five binding sites for sequence-

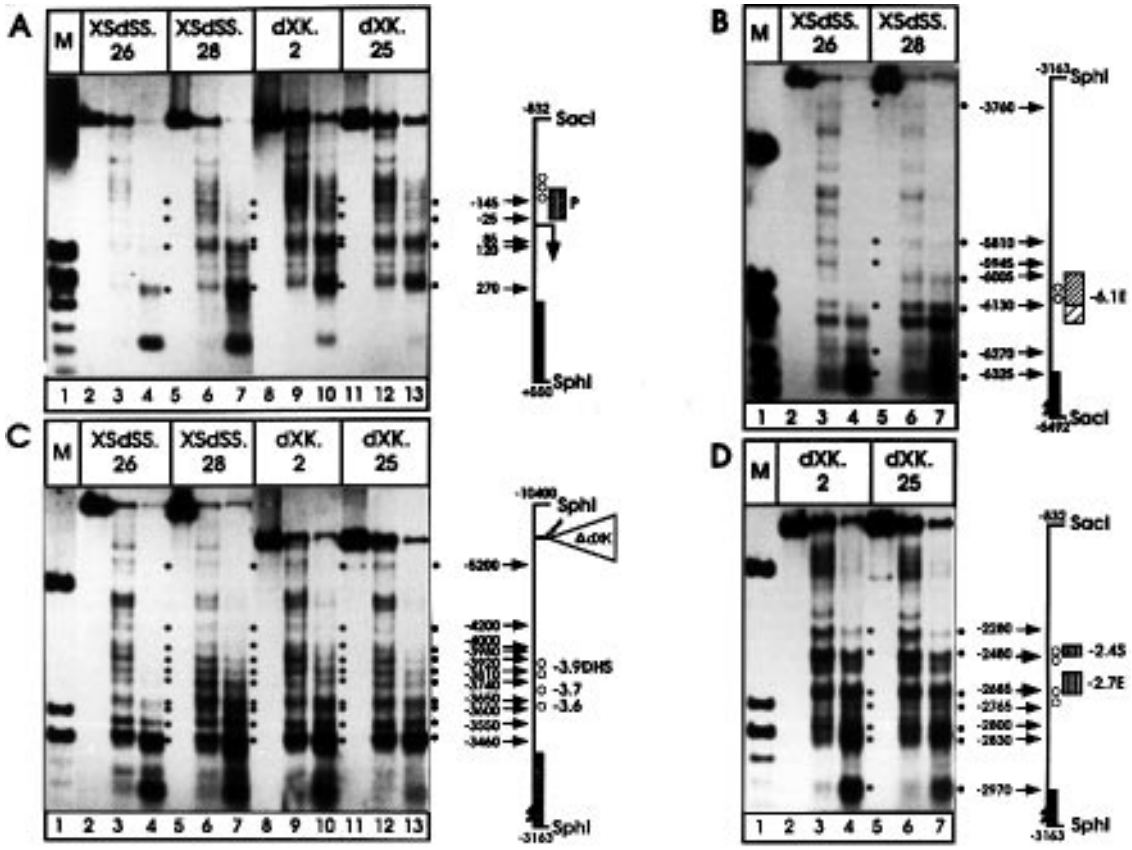

Figure 6. MNase analysis of lysozyme transgene chromatin in position dependently expressing mouse lines. Nuclei from macrophages of the indicated mouse lines were digested with MNase and DNA was analyzed as described. The maps [(A)–(D) at the right] display all chromatin specific MNase cuts detectable in macrophages of the various transgenic mouse lines. (**A**) Promoter region. Genomic DNA was digested with *Sph*I and *Sac*I, probe 1 was used for indirect endlabelling. (**B**) Upstream enhancer region. Genomic DNA was restricted with *Sph*I and *Sac*I and analyzed as described in Figure 4. (**C**) –3.9 kb DHS region. DNA was restricted with *Sph*I and analyzed as described in Figure 3. The position of the deletion in dXK mice is indicated by a triangle in the map. (**D**) Medial enhancer region. Genomic DNA was restricted with *Sph*I and *Sac*I and analyzed as described in Figure 2. For explanation of all other symbols: see legend of Figure 1.

specific DNA-binding proteins. *In vitro* binding assays showed binding of NFI at –6000 bp and of C/EBP to two sites at –5900 and –5943 bp (29,46–48). 5′ of the minimal enhancer fragment a second NFI binding site at –6192 bp is present, whose role in transcriptional activation has not been examined. *In vivo* G(N7) protein contacts in HD11 cells have been mapped at each of the two NFI sites and the downstream C/EBP site (49). The chromatin of the –6.1 kb enhancer region in inactive cells exhibits a regular pattern of MNase cleavage sites (Fig. 4A, lanes 5–10; Fig. 4B, lanes 2–4), indicating the presence of at least one phased nucleosome which is precisely located over the enhancer element as indicated by two prominent MNase cuts at –5945 and –6130 bp. Upon transcriptional activation the nucleosome positioned over the enhancer element is rearranged. Instead of a sharp band at the 3′ border of the enhancer around –5945 bp, two new MNase generated bands at –6005 and –6030 bp appear. At the 5′ border of the enhancer element upstream of the NFI site at –6130 bp a previously weak band increases in strength (Fig. 4A, lanes 11–19). Unlike at the –2.7 kb enhancer, the DHS analysis performed for comparison (Fig. 4B, lane 8) indicates the co-localization of DHS and enhancer element.

The chromatin structure of position dependently expressed transgene-clusters is heterogeneous

The majority of transgenes generated by direct transfer of DNA into cells are inserted as multiple copies at random positions into the genome. With position dependently expressed transgenes in different mouse lines variable expression levels per gene copy are observed with the same construct. The various lysozyme locus constructs and their expression levels per gene copy in transgenic mice are depicted in Figure 5. Our previous experiments had pointed to a structural difference within multiple transgene loci (19,23). However, another possibility was a distortion of nucleosome positioning in mouse lines carrying *cis*-regulatory deletions and expressing the gene at a low level per gene copy, thus inhibiting DHS formation.

We compared the nucleosomal organization of the various *cis*-acting elements in macrophages of different position dependently expressing mouse lines (Fig. 6). No fundamental change in chromatin structure is observed as compared with the position independently expressing mouse lines. At the promoter (Fig. 6A) all position dependently expressing mouse lines show a

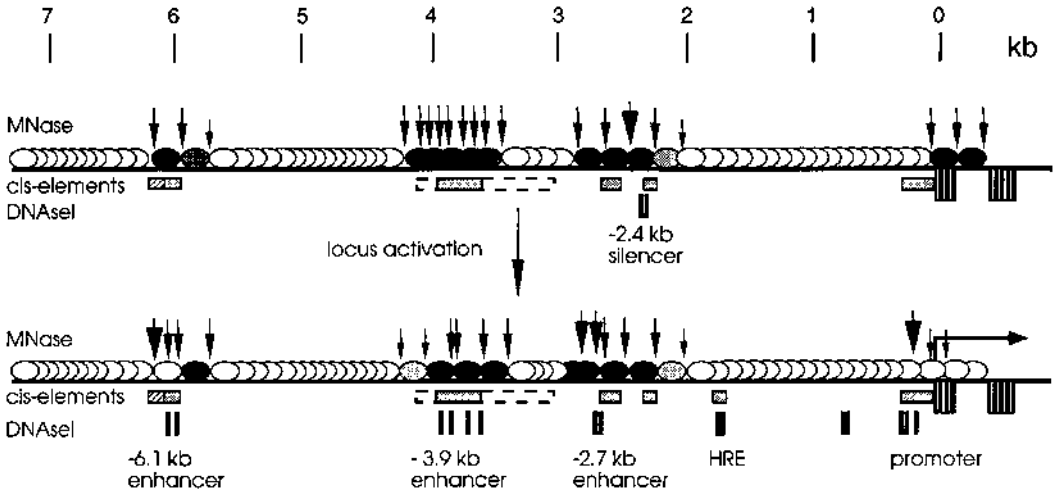

Figure 7. Nucleosomal organization of the chicken lysozyme locus 5′-regulatory region. Exons are indicated as striped boxes. The positions of *cis*-regulatory elements are depicted as light grey boxes. The –3.9 kb enhancer has up to now only been identified by testing a 1.6 kb fragment (indicated with stippled lines) in transient transfection assays. DHSs are indicated as black bars. The positions of chromatin specific MNase cuts are indicated as black arrows, MNase hypersensitive sites are shown as large black arrows. Black circles represent phased nucleosomes as indicated by a regular 150–200 bp distance of MNase cuts; light grey circles indicate nucleosomes most likely phased, but flanked by weak MNase sites; grey circles indicate specific MNase cuts indicating alternative nucleosomal positions; white circles indicate areas with no prominent MNase cleavage sites where nucleosomes are placed randomly or have been destabilized. The upper panel shows the positions of phased nucleosomes in non-expressing cells, the lower panel shows the nucleosomal pattern found in fully transcriptionally active cells.

mixed MNase pattern. Both, the MNase cleavage site at –145 bp, which is indicative for an activated promoter as well as the cleavage sites at –25 bp and +120 bp indicative for an inactive promoter structure are present (compare with Fig. 1A and B). Chromatin analysis was carried out with nuclei of mouse macrophages from the same differentiation stage, hence, a mixed MNase cleavage pattern is an indication of a structural heterogeneity between transgene copies. The comparison of MNase cleavage patterns at the –6.1 kb enhancer region revealed more pronounced differences (compare Fig. 6B with Fig. 4B, lanes 2–7). Mouse lines XSdSS.26 and 28 carry a deletion of the medial enhancer region. Macrophages of the low expressing mouse line XSdSS.26 exhibit the MNase cleavage pattern observed in transcriptionally inactive cells (compare Fig. 6B, lanes 2–4 with Fig. 4B, lanes 2–4), the high expressing mouse line XSdSS.28 shows a mixed pattern with a significant number of gene copies in the active structural configuration of the *cis*-element (compare Fig. 6B, lanes 5–7 with Fig. 4B, lanes 5–7). A similar observation was made when the –3.9 kb region was analyzed (compare Fig. 6C with Fig. 3B, lanes 5–7). The low expressing mouse line (dXK.25) and a higher expressing mouse line (dXK.2) carry a transgene with a deletion of the –6.1 kb enhancer region (Fig. 6C, lanes 8–13). In this experiment the –3.9 kb region exhibits a mostly inactive (XSdSS.26) or a mixed (XSdSS.28; dXK.25; dXK.2) configuration.

The medial enhancer region was analyzed in mouse lines dXK.2 and dXK.25 (Fig. 6D). In both cases a mixed pattern is observed. The MNase cleavage site upstream of the silencer element at –2480 bp is less accessible than in transcriptionally inactive cells, resembling the pattern found in transcriptionally active cells. Upstream of the enhancer element staggered MNase cleavage sites are visible reminiscent of the mixed pattern seen in myeloblasts (Fig. 2A) and indicating the presence of very few gene copies in the active configuration of the enhancer. Here, no strict correlation between transcriptional activity and transgene organization is found, implicating some extent of autonomy of the medial enhancer region with respect to chromatin reorganization. A molecular explanation for this result might be provided by the recent finding, that the thyroid hormone receptor, one of the proteins binding to the –2.4 kb silencer, exhibits constitutive binding to chromatin in the absence of ligand and reorganizes chromatin upon ligand binding (11). In summary, our results confirm the hypothesis that chromosomal position effects result in a structural heterogeneity of gene loci within a multi-copy transgene cluster.

DISCUSSION

The various *cis*-regulatory elements of the chicken lysozyme locus remodel chromatin differently

The chromatin of the 5′-regulatory region of the chicken lysozyme locus is highly structured and is gradually rearranged during cellular differentiation (Fig. 7). In transcriptionally inactive cells the –6.1 kb enhancer is covered by a phased nucleosome. The –2.4 kb silencer/–2.7 kb enhancer region is covered by an array of four positioned nucleosomes which occupy almost 1 kb of DNA. At the promoter nucleosomes are placed upstream and downstream of the main transcriptional start site. In contrast, the area around the –3.9 kb enhancer does not show a distinct nucleosomal phasing pattern.

Transcriptional activation results in significant rearrangements of chromatin structure, which, however, are of different nature, depending on the *cis*-regulatory element (Fig. 7). At the promoter a DHS is formed in a region where transcription factors bind *in vivo*. The phased nucleosome at the transcriptional start site is destabilized. The formation of a MNase hypersensitive site at position –145 bp downstream of the DHS is therefore an indication for the presence of a large DNA–protein complex around –200 bp, with the nuclease cleaving at its 3′ border. DNase I, whose action is less affected by protein–DNA interactions (50), recognizes structural changes in chromatin around the factor-binding sites.

Transcription factor binding to the –3.9 kb stimulatory element leads to phasing of nucleosomes around the DHS.

Transcription factor binding at the –6.1 kb enhancer leads to its increased accessibility towards MNase digestion. DNase I recognizes the very same area. Therefore, our results indicate a remodelling of the nucleosomal structure, rendering a short region of ~70 bp of DNA accessible to the action of both enzymes. Upstream of the minimal enhancer element, at –6130 bp, a MNase hypersensitive site develops, indicating that nucleosome remodelling might render the linker region more accessible. Alternatively, a large non-nucleosomal DNA–protein complex might form, changing chromatin structure between the two NFI sites located on either side of the MNase hypersensitive site.

At the medial enhancer region the silencer complex forms a DHS on the surface of a phased nucleosome, probably weakening its interaction with DNA and thus generating a MNase hypersensitive site at its 5′ border. The distance between factor binding sites of the silencer and the enhancer indicate that both are facing the same site on the surface of each nucleosome. The protein complex binding to the silencer might thus interfere with binding of transcription factors at the enhancer. Transcriptional activation does not result in a displacement of the nucleosome located at the –2.7 kb enhancer element. Instead, MNase- and DNase I-hypersensitive sites at the silencer disappear, indicating the loss of binding factors. As a result enhancer specific factors may be free to bind thus rendering chromatin accessible to DNase I at the 5′ border of the underlying nucleosome and in the neighboring linker region. We suggest that a protein–DNA complex consisting of both histones and transcription factors restricts MNase as well as DNase I action. MNase cleaves at the outer borders of this large complex, whereas DNase I recognizes sequences closer to the transcription factors binding sites. Our results point towards a highly complex chromatin structure of this region which undergoes extensive changes during development. From our results it is likely that the correct function of the –2.4 kb/–2.7 kb silencer/enhancer region requires the interaction and precise alignment of phased nucleosomes and transcription factors.

Our experiments implicate a pronounced influence of chromatin structure on transgene expression. We suggest that the unique chromatin organization of each *cis*-regulatory element is required for the correct functioning of the lysozyme locus as a whole. Experimental evidence for this assumption is provided by experiments with transgenic mice. Constructs comprised of short fragments encompassing the minimal regulatory regions are not expressed (Bonifer, C., Vidal, M., Grosveld, F. and Sippel, A.E., unpublished results). One of the reasons for this finding might be that such constructs fail to support the gradual chromatin rearrangements necessary to activate the gene locus during cell differentiation. Steric hindrance may inhibit the correct alignment of nucleosomes necessary for the correct functioning of *cis*-regulatory elements.

Multi-copy clusters of position dependently expressed transgenes exhibit a heterogenous chromatin structure

The complete chicken lysozyme locus is correctly regulated in the mouse and its original nucleosomal organization is reformed in the new host. This allowed us to examine the chromatin structure of a multi-copy transgene cluster when its expression is disturbed by chromosomal position effects. We find that such transgenes exhibit a variable ability to perform nucleosome rearrangements. Depending on the chromatin environment a variable number of genes within each multi-copy gene cluster develop an active chromatin structure.

The structural consequences of the chromosomal position effects we describe differ from what is found with classical position effect variegation (PEV) phenomena (51,52). Also here transgene chromatin structure is altered as compared with non-variegating transgenes (53), whereby transgenes are silenced by the spreading of juxtaposed heterochromatin (54–56). Each cell exhibits a different level of expression, indicating that in each of them heterochromatin has spread over variable distances. In the mouse similarly heterogenous transgene expression levels in cells of one mouse strain have been observed (57,58). A reason for this result could be interactions between multiple transgene copies. An apparent position independence of expression was observed with multi-copy transgenes containing only a few transcription factor binding sites, suggesting compensatory interactions between different loci within the same transgene cluster (59). Once the constructs are severely crippled, position independence of expression is lost, but interactions may still proceed with variable efficiencies in different cells. It was suggested that somatic pairing between multiple transgenes can induce heterochromatization (60). However, with lysozyme transgenes position independence of expression is lost whenever one *cis*-regulatory element is deleted. The degree of suppression of expression is not correlated to transgene copy number (19). An explanation for our finding might be that the –6.1 kb enhancer, the –3.9 kb enhancer and the –2.7 kb enhancer are not equivalent and their lack on one gene copy can not be compensated by the presence of the same element on a neighboring gene copy. Our results support this idea, each *cis*-regulatory element reorganizes chromatin in its unique fashion. At each element transcription factors might be uniquely aligned, thus allowing only cooperative, but not compensatory interactions. Our data show that once interactions are excluded, transgenes in multi-copy clusters act as isolated individual units, their activation being solely influenced by the equilibrium between silencing factors of the surrounding chromatin and activating factors bound to the transgene.

ACKNOWLEDGEMENTS

This work was supported by a grant from the Deutsche Forschungsgemeinschaft to C.B. The authors want to thank Thomas Graf, EMBL for providing the chicken cell lines as well as Albrecht E. Sippel, Nicole Faust and Albrecht Müller for helpful discussions and comments on the manuscript.

REFERENCES

1 Thoma, F. (1992) *Biochim. Biophys. Acta*, **1130**, 1–19.
2 Felsenfeld, G. (1992) *Nature*, **255**, 219–224.
3 Durrin, L.K., Mann, R.K., Clayne, P.S. and Grunstein, M. (1991) *Cell*, **65**, 1023–1031.
4 Johnson, L.M., Fisher-Adams, G. and Grunstein, M. (1992) *EMBO J.*, **11**, 2201–2209.
5 Thompson, J.S., Ling, X and Grunstein, M. (1994) *Nature*, **369**, 245–247.
6 Fascher, K.D., Schmitz, J. and Hörz, W. (1993) *J. Mol. Biol.*, **231**, 658–667.
7 Wall, G., Varga-Weisz, P.D., Sandaltzopoulos, R. and Becker, P. (1995) *EMBO J.*, **14**, 1727–1736.
8 Pina, B., Brüggemeier, U. and Beato, M. (1990) *Cell*, **60**, 719–731.
9 Taylor, I.C.A., Workman, J.L., Schuetz, T.J. and Kingston, R.E. (1991) *Genes Dev.*, **5**, 1285–1298.
10 Richard -Foy, H. and Hager, G.L. (1987) *EMBO J.*, **6**, 2321–2328.
11 Wong, J., Shi, Y.-B. and Wolffe, A.P. (1995) *Genes Dev.*, **9**, 2696–2711.

12 Truss, M., Bartsch, J., Schelbert, A., Hache, R.J.G. and Beato, M. (1995) *EMBO J.*, **14**, 1737–1751.
13 Fragoso, G., John, S., Roberts, M.S and Hager, G.L (1995) *Genes Dev.*, **9**, 1933–1947.
14 Li, Q. and Wrange, Ö. (1995) *Mol. Cell. Biol.*, **4375**, 4384.
15 McPherson, C.E., Shim, E.-Y., Friedman, D.S. and Zaret, K. (1993) *Cell*, **75**, 387–398.
16 Alevy, M.C., Tsai, M.J. and O'Malley, B.W. (1984) *Biochemistry*, **23**, 2309–2314.
17 Jantzen, K., Fritton, H.P. and Igo-Kemenes, T. (1986) *Nucleic Acids Res.*, **14**, 6085–6099.
18 Bonifer, C., Vidal, M., Grosveld, F. and Sippel, A.E. (1990) *EMBO J.*, **9**, 2843–2848.
19 Bonifer, C., Yannoutsos, N., Krüger, G., Grosveld, F. and Sippel, A.E. (1994) *Nucleic Acids Res.*, **22**, 4202–4210.
20 Fritton, H.P., Sippel, A.E. and Igo-Kemenes, T. (1983) *Nucleic Acids Res.*, **11**, 3467–3485.
21 Fritton, H.P., Igo-Kemenes, T., Nowock, J., Strech-Jurk, U., Theisen, M. and Sippel, A.E. (1984) *Nature*, **311**, 163–165.
22 Fritton, H.P., Igo-Kemenes, T., Nowock, J., Strech-Jurk, U., Theisen, M. and Sippel, A.E. (1987) *Biol. Chem.* Hoppe-Seyler, **368**, 111–119.
23 Huber, M.C., Bosch, F., Sippel, A.E. and Bonifer,C. (1994) *Nucleic Acids Res.*, **22**, 4195–4201.
24 Noll, M. (1974) *Nature*, **251**, 249–251.
25 Metz, T. and Graf, T. (1991) *Genes Dev.*, **5**, 369–380.
26 Beug, H., v.Kirchbach, A., Döderlein, G., Conscience, J.-F. and Graf, T. (1979) *Cell*, **18**, 375–390.
27 Baniahmad, A., Müller, M., Steiner, C. and Renkawitz, R. (1987) *EMBO J.*, **6**, 2297–2303.
28 Baniahmad, A., Müller, M., Steiner, C. and Renkawitz, R. (1990) *Cell*, **61**, 729–740.
29 Grewal, T., Theisen, M., Borgmeyer, U., Grussenmeyer, T., Rupp, R.A.W., Stief, A., Qian, F., Hecht, A. and Sippel,A.E. (1992) *Mol. Cell. Biol.*, **12**, 2339–2350.
30 Hecht, A., Berkenstam, A., Strömstedt, P.-E., Gustafsson, J.-A. and Sippel, A.E. (1988) *EMBO J.*, **7**, 2063–2073.
31 Steiner, C., Müller, M., Baniahmad, A. and Renkawitz, R. (1987) *Nucleic Acids Res.*, **15**, 4163–4178.
32 Theisen, M., Stief, A. and Sippel, A.E. (1986) *EMBO J.*, **5**, 719–724.
33 Ahne, B. and Strätling, W.H. (1994) *J. Biol. Chem.*, **269**, 17794–17801.
34 Graf, T., McNagny, K., Brady, G. and Frampton, J. (1992) *Cell*, **70**, 201–213.
35 Huber, M.C., Graf, T., Sippel, A.E. and Bonifer, C. (1995) *DNA Cell. Biol*, **14**, 397–402.
36 Saueressig, H. (1994) PhD thesis. University of Freiburg,
37 Grez, M., Land, H., Giesecke, K., Schütz, G., Jung, A. and Sippel, A.E. (1981) *Cell*, **25**, 743–752.
38 Dölle, A. and Strätling, W.H. (1990) *Gene*, **95**, 187–193.
39 McKnight, S.L. (1992) In McKnight, S.L. and Yamamoto, K.R. (eds) *Transcriptional Regulation.* Cold Spring Harbor Laboratory Press, Cold Spring Harbor, NY. pp. 771–795.
40 Natsuka, S., Akira, S., Nishio, Y., Hashimoto, S., Sugita, T., Isshiki, H. and Kishimoto, T. (1992) *Blood*, **79**, 460–466.
41 Sippel, A.E., Theisen, M., Borgmeyer, U., Strech-Jurk, U., Rupp, R.A.W., Püschel, A.W., Müller, A., Hecht, A., Stief, A. and Grussenmeyer,T. (1988) In Kahl, G. (ed.) *The Architecture of Eukaryotic Genes.* Verlagsgesellschaft Chemie (VHC), Weinheim, pp. 355–369.
42 Köhne, A.C., Banaihmad, A. and Renkawitz, R. (1993) *J. Mol. Biol.*, **232**, 747–755.
43 Müller, A., Grussenmeyer, T., Strech-Jurk, U., Theisen, M., Stief, A. and Sippel, A.E. (1990) *Bone Marrow Transplant.*, **5**, 13–14.
44 Altschmied, J., Müller, M., Baniahmad, S., Steiner, S. and Renkawitz, R. (1989) *Nucleic Acids Res.*, **17**, 4975–4991.
45 Goethe, R. and Phi van, L. (1994) *J. Biol. Chem.*, **269**, 31302–31309.
46 Nowock, J. and Sippel, A.E. (1982) *Cell*, **30**, 607–615.
47 Borgmeyer, U., Nowock, J. and Sippel, A.E. (1984) *Nucleic Acids Res.*, **12**, 4295–4311.
48 Sippel, A.E., Borgmeyer, U., Püschel, A.W., Rupp, R.A.W., Stief, A., Strech-Jurk, U. and Theisen, M. (1987) In Hennig, W. (ed.) *Results and Problems in Cell Differentiation.* Springer-Verlag, Berlin Heidelberg, Vol. 14. pp. 255–269.
49 Sippel, A.E., Stief, A., Hecht, A., Müller, A., Theisen, A., Borgmeyer, U., Rupp, R.A.W., Grewal, T. and Grussenmeyer, T. (1989) In Eckstein, F. and Lilley, D.M.J. (eds) *Nucleic Acids and Molecular Biology.* Springer Verlag, Berlin Heidelberg, Vol. 3. pp. 133–147.
50 Noll, M. (1974) *Nucleic Acids Res.*, **1**, 1573–1586.
51 Shaffer, D.C., Wallrath, L.L. and Elgin, S.C.R. (1993) *Trends Genet.*, **2**, 35–37.
52 Henikoff, S. (1990) *Trends Genet.*, **6**, 422–426.
53 Wallrath, L.L. and Elgin, S.C.R. (1995) *Genes Dev.*, **9**, 1263–1277.
54 Allshire, R.C., Javerzat, J.P., Redhead, N.J. and Cranston, G. (1994) *Cell*, **76**, 157–169.
55 Renauld, H., Aparicio, O.M., Zierath, P.D., Billington, B.L., Chhablani, S.K. and Gottschling, D.E. (1993) *Genes Dev.*, **7**, 1133–1145.
56 Gottschling, D.E., Aparicio, B.L., Billington, B.L. and Zakian, V.A. (1990) *Cell*, **63**, 751–762.
57 Elliot, J.I., Festenstein, R., Tolani, M. and Kioussis,D. (1995) *EMBO J.*, **14**, 575–584.
58 Robertson, G., Garrock, D., Wu, W., Kearns, M., Martin, D. and Whitelaw, E. (1995) *Proc. Natl Acad. Sci. USA*, **92**, 5371–5375.
59 Ellis, J., Talbot, D., Dillon, N. and Grosveld, F. (1993) *EMBO J.*, **12**, 127–134.
60 Dorer, D.R. and Henikoff, S. (1994) *Cell*, **77**, 993–1002.